Gasoline direct injection engine soot oxidation: fundamentals and determination of kinetic parameters

Bogarra Macias, Maria; Herreros, Jose; Tsolakis, Athanasios; Rodriguez-Fernandez, Jose; York, Andrew ; Millington, Paul

DOI:
10.1016/j.combustflame.2017.11.027

Gasoline Direct Injection Engine soot oxidation: fundamentals and determination of kinetic parameters

M. Bogarra[a], J.M. Herreros[a], A. Tsolakis[a*], J. Rodríguez-Fernández[b], A.P.E. York[c], and P.J. Millington[c]

[a]*Mechanical Engineering, University of Birmingham, Edgbaston, B15 2TT, UK*

[b] *Escuela Técnica Superior de Ingenieros Industriales, University of CastillaLa Mancha, Edificio Politécnico, Avenida Camilo Jose Cela,s/n, 13071 Ciudad Real, Spain*

[c]*Johnson Matthey Technology Centre, Blount's Court, Sonning Common, Reading, RG4 9NH, UK*

*Corresponding author. Tel.: +44 (0) 121 414 4170. E-mail address: a.tsolakis@bham.ac.uk (A. Tsolakis).

ABSTRACT

Current emissions legislation for road transport vehicles, including modern gasoline vehicle fleet limits the mass and the number of Particulate Matter (PM) emitted per kilometre. The introduction of a gasoline particulate filter (GPF) is expected to be necessary, as was the case for diesel vehicles, the traditionally recognised source of PM in transportation. Therefore, for the design of efficient GPFs and the regeneration strategies, soot oxidation characteristics in gasoline must be understood.

Extensive research has been carried out mainly to investigate the oxidation of diesel soot, however, in the most cases soot were collected on microfiber filters and the activation energy was calculated with the logarithm method assuming mass and oxygen reaction orders equal to one. Identified limitations that lead to inconsistent and inaccurate trends and results are presented in this paper. As a consequence, a novel methodology to accurately obtain the oxidation kinetic parameters for soot emitted from a Gasoline Direct Injection (GDI) engine has been developed and presented in this paper. The particles collected in a silicon carbide wall-flow particulate filter are directly exposed to oxidation conditions in a thermogravimetric analysis (TGA) without the use of microfiber filter.

The significance of more accurate and consistent calculations of soot oxidation kinetic parameters as a result of this methodology will aid modelling and experimental work of the aftertreatment systems and will lead in improving the GPF regeneration process in modern GDI vehicles. Avoiding high peak temperatures during regeneration and large thermal stress gradients and thus increasing the operating life of the filters is amongst the benefits can be seen.

Keywords: soot oxidation, pollution, activation energy, gasoline engines, particulate matter, thermogravimetric analysis

1. INTRODUCTION

Particulate matter (PM) emissions are composed of a carbonaceous core, known as soot, onto which different hydrocarbon species, especially polyaromatic hydrocarbons (PAHs), can be adsorbed.

Internal combustion engines are the main source of PM. Although the introduction of Gasoline Direct Injection (GDI) has proven to be an efficient technology capable of significantly reducing fuel consumption and CO_2 emissions from road transport vehicles, its wider implementation has also raised interest due to the increase in PM emissions [1, 2].

In general the effect of PM in the environment and on human health is diverse; it is reported to cause building soiling and reduced visibility after high PM level episodes [3]. Moreover, PM can penetrate into the human body through the respiratory system causing asthma, bronchitis or exacerbating allergies [4]. From the lungs, PM can spread to different organs, such as the liver or brain, through the blood stream [5]. PM can block the arteries increasing stroke risk and provoking cardiovascular-related complications [6]. As the awareness of the deleterious effects of PM is increasing, stricter limitations are being imposed to gasoline and diesel powered road vehicle, including the Euro 6c which will limit PM levels to $6x10^{11}$ particles per kilometre.

One of the most widely used techniques to obtain oxidation rate parameters is thermogravimetric analysis (TGA). In diesel engines, extensive efforts have been made to characterise the kinetic parameters of soot in both non-catalysed [7] and catalysed samples [8, 9]. Understanding and modelling the soot oxidation processes can provide useful data for automotive engineers to design optimised strategies for filter regeneration, saving fuel and extending the catalyst's life, as well as reducing local temperature peaks in the catalyst. Studies performed in diesel engines shown that the particle oxidation characteristics can be influenced by the particle morphology (i.e. primary particle size, fractal dimension), particle nanostructure (size of the graphene layers and curvature) as well as particle composition [10-12]. However, in GDI engines this knowledge is still not well established and the different local in-cylinder conditions might result in different particle characteristics. TGA has been used to quantify the composition of PM: volatile organic compounds (VOC)/soot ratio and ash percentage [13, 14], and to prepare the PM sample for subsequent studies [14, 15]. For instance in [15], soot samples were partially oxidised under 8% oxygen and 1000 and 2000 ppm NO_2 in 8% oxygen to examine the physicochemical properties of soot during the oxidation process through Transmission Electron Microscope (TEM).

There are a limited number of studies on soot oxidation kinetics in the literature to date. These studies mainly focus on the effects of fuel and engine operating condition on activation energy and reaction order for soot oxidation. Luo et al. [16] analysed the activation energy for soot samples derived from gasoline, E10 and E20 blends under four different operating engine conditions using the Arrhenius-like equation logarithm method and assuming first reaction order for mass and oxygen. The activation energy for gasoline soot was found to lie between 197 and 256 $kJ \cdot mol^{-1}$ whereas for ethanol blends soot, higher oxidative reactivity was reported. E10 activation energy was in the range of 183 to 221 $kJ \cdot mol^{-1}$ and E20 from 163 to 189 $kJ \cdot mol^{-1}$. Higher activation energies and higher oxidation temperatures were found for higher engine loads that the authors hypothesised were on account of the

greater ordered structures. Wang et al. [17] analysed the PM composition and soot characteristics under two different engine conditions using a single cylinder engine fuelled with gasoline, ethanol and 2,5-dimethylfuran (DMF). The effect of the heating ramp and sample load was analysed in order to develop a TGA methodology for GDI soot. The kinetic parameters were obtained using the logarithm method, again assuming one for both reaction orders. The activation energy found for gasoline soot was 131 and 153 $kJ \cdot mol^{-1}$ at 1500 rpm, 5.5 and 8.5 bar indicated mean effective pressure (IMEP) respectively. Ethanol and DMF were also reported to reduce the activation energy of soot oxidation when compared to gasoline. Due to the low oxygen concentration present in the gasoline exhaust, it is important to estimate the oxygen reaction order to predict the soot oxidation behaviour in actual gasoline exhaust environment. In the majority of the investigations carried out for diesel soot, reaction order one for both oxygen and mass has been assumed, while for GDI engines, several investigations have estimated the reaction orders in order to separate the effect of mass and oxygen concentration. Wang-Hansen et al. [18] analysed the reactivity and kinetics of particles emitted by diesel, gasoline Port Fuel Injection (PFI) and GDI soot in comparison to a Printex U reference. Temperature programmed oxidation and isothermal experiments were carried out under different concentrations of oxygen and NO_2. The reported activation energy for GDI soot was 146 $kJ \cdot mol^{-1}$ and similar to soot from PFI engines [9], and both were higher than diesel soot. On the other hand, ethanol soot was reported to be more reactive. Choi et al. [19] calculated the activation energy, prefactor and mass reaction order of GDI soot samples under five different engine conditions following the Arrhenius-like equation logarithm method. The activation energy ranged from 125 to 142 $kJ \cdot mol^{-1}$, the prefactor from 13500 and 127000 s^{-1} and the mass reaction order from 0.512 to 1.011. The authors in [19] did not find any correlation between the engine operating condition and the kinetic parameters while a catalytic effect of the ash was observed in the GDI soot oxidation process.

A summary of the kinetic parameters reported in the literature is presented in Table 1. The activation energy of gasoline soot lies in the wide range between 125 and 256 $kJ \cdot mol^{-1}$ depending on engine operation condition, fuel formulation, soot collection and soot reactivity method. This is a similar activation energy window to that reported for diesel soot in the literature, 100-300 $kJ \cdot mol^{-1}$ [20]. There is an agreement in the literature that the microstructure of soot emitted from gasoline engines is less ordered than the microstructure of diesel soot [14], whereas the effects of engine speed and load are not fully understood yet [19]. It is also reported that soot produced under ethanol combustion has higher soot reactivity compared to gasoline soot. The authors claimed that ethanol enhanced the oxidation activity due to i) smaller particle size and ii) more disordered microstructure [16]. It has also to be noted, the lower concentration of oxygen in a gasoline exhaust could become a challenge for particulate filter regeneration, thus further analysis is needed to understand GDI soot characteristics.

The aim of this research work is to develop a new robust methodology in order to obtain accurate and consistent information of the GDI soot oxidation parameters such as activation energy, prefactor, mass

reaction order and oxygen reaction order. The first section of the paper studies the capabilities and limitations of the state of the art particle collection methods where microfiber filters are used to collect particles under different engine exhaust conditions. Based on the identified limitations of the methodologies in the first section of the paper in the second section particles are collected in a vehicle exhaust particulate filter to better reproduce the oxidation process in the actual aftertreatment system, and were then removed for direct exposure to the TGA analysis. Soot oxidation kinetic parameters are estimated using the Arrhenius-like equation and assessed and compared to the proposed methodology using isothermal processes instead of heating ramps. The proposed particles collection method and methodology enable to characterise the gasoline soot oxidation parameters under gasoline-like environments to understand particle filter regeneration processes in GDI engines.

Table 1. Summary of the kinetic parameters found in the literature.

2. STUDY OF THE INFLUENCE OF MICROFIBER FILTERS IN SOOT OXIDATION

2.1. Experimental setup

The engine used for this study is a 2 L, 4-cylinder, air-guided GDI. A steady-state condition corresponding to a medium-load stage of the NEDC was selected: 2100±2 rpm and 4.7±0.3 bar IMEP. The details of the engine specification can be found in Table 2. Standard EN228 gasoline provided by Shell has been used for this research. Fuel properties are presented in Table 3. The fuel injection timing was advanced to 335 CAD bTDC enhancing soot formation (as it has been previously reported in [21, 22]) to accelerate the loading process and obtain a sufficient amount of soot for the TGA.

Table 2. Engine specifications.

Table 3. Gasoline properties.

2.2. Established experimental methods and test procedure

This section describes available TGA methodology that has extensively been use in characterising diesel engine soot [7, 23-27] and more recently was also applied in characterising soot from GDI engines [16, 17].The kinetic parameters are estimated by taking logarithms on the formal Arrhenius-like kinetic equation (Equation 1). Although there is still no consensus about the value of the mass and oxygen reaction order, the majority of studies assume order one for oxygen partial pressure and soot mass [16, 17, 23, 28] or estimate the product $A' = A \cdot p_{O_2}^r$ without identifying the oxygen reaction order.

$$-\frac{dm}{dt} = A \cdot p_{O_2}^r \cdot e^{\frac{-E_a}{RT}} \cdot m^n = A' \cdot e^{\frac{-E_a}{RT}} \cdot m^n \quad [1]$$

Where m is the mass of the soot sample, t, the time, E_a, the activation energy for soot oxidation, R, the universal gas constant (8.314 J·mol^{-1}·K^{-1}), T, the sample temperature and n and r are the soot and oxygen reaction orders respectively. This form m^n is generally acceptable and often applied by researchers for heterogeneous thermal processes such as soot oxidation [23]. Further details of the methodology employed can be found in a previous work of the authors [21].

Whatman GF/F Glass microfiber 47 mm diameter filters were loaded in the diluted exhaust (dilution ratio DR=11±1 and 45ºC±5) at different soot concentration levels with respect to the baseline condition i) using 24 % (v/v) exhaust gas recirculation (EGR) and ii) 24% (v/v) reformed exhaust gas recirculation (REGR) where hydrogen and CO are present in the EGR loop. Further details of the REGR technique can be found in [21]. The filters were pre-heated at 600ºC during 6 hours to limit any influence of filter material losses during the nitrogen phase in the TGA. Firstly, all the filters were

loaded during a constant time (one hour) to independently study the influence on soot oxidation of collecting different quantities of particles in accord with the particle exhaust concentration. The results are also compared for different loading times of the microfiber filter, but with similar mass of particles loaded (i.e. using exhaust from different engine condition) on the filter material. In order to avoid any loss of particles during the sampling process, instead of scratching the filters, a sharp cylindrical hollow pipe was used to cut filter portions.

A TG analyser, model Pyris 1 from Perkin Elmer, has been used for the experimental analysis to estimate the soot oxidation kinetic constants. The temperature precision of the TGA furnace is ±5ºC and the microbalance precision is 0.001%. The TGA test procedure is summarized in Table 4 and Figure 1. A heating ramp of 3°C/min was used for both heating and cooling steps; it was found that this value is a compromise between the duration of the test and the complete oxidation of the sample [17]. Prior to the test, the sample was maintained in a nitrogen atmosphere at 40°C in order to avoid the effect of ambient temperature fluctuations and increased until 450°C with the aforementioned heating ramp to remove VOC content. Then, the furnace was cooled down to 150°C in order i) to obtain a symmetric process to the VOC removal for the soot oxidation and ii) to increase the soot oxidation temperature window [17]. After the inert atmosphere process, the sample was exposed to an oxidant atmosphere in order to oxidise the soot. This process was again carried out at 3°C/min. A pressurised air bottle (21% oxygen in nitrogen) was used for this analysis. A nitrogen balance flow (99.999% oxygen free nitrogen) is required by the equipment to assure i) the proper inert environment of the microbalance and ii) prevents volatile and combustion gases from back-streaming into the microbalance area. The air (40 mL/min) and balance flow rates (60 mL/min) were kept constant during all experiments at the values recommended by the TG analyser manufacturer and different synthetic oxygen in nitrogen concentrations were used. For the Pyris 1, the balance flow will reduce the oxygen concentration in the furnace from the 21% concentration supplied by the pressurized air bottle. Therefore, the oxygen concentration was measured inside the TG furnace. A 10 L Supel Inert Multi-Layer Foil Gas Sampling bag was connected to the exhaust line of the TG analyser for about three hours. When enough volume was collected, the bag was connected to an AVL 440 Digas non-dispersive infrared analyser to measure the oxygen concentration (electrochemical method) inside the TG analyser furnace: 16.6% oxygen was obtained.

Table 4. TGA program.

Figure 1. TGA program.

2.3. Experimental Results

2.3.1. Effect of soot concentration on its oxidation characteristics

The results corresponding to constant particle loading time (one hour) in the microfiber filters are presented in Figure 2. The area under the curves in the figure is proportional to the mass of soot collected on the filters, which is different in the three engine test modes (i.e. EGR, REGR). In the case of the baseline condition (i.e. noEGR) the maximum mass loss rate temperature (MMLRT), which is often used as a parameter for soot reactivity, is shifted to higher temperature with respect to those obtained from the soot produced under EGR and REGR combustion. This could have been interpreted as an indicator of the easier oxidation of the soot produced under EGR and REGR. However, Figure 2 also shows that the weight loss derivative remained constant for the three cases until the temperature reached 510°C. This suggests that the different trends in oxidation behaviour are a mass artefact rather than a difference in the nature of the particles collected under the different conditions investigated.

Figure 2. Effect of EGR and REGR on soot oxidation rate in TGA.

In order to calculate the activation energy, the logarithm method widely applied in the literature for soot oxidation: a reaction order of one for both mass and oxygen concentration was used to calculate the activation energy of the particulates. The resulting activation energy of 100 kJ/mol [21], was reported in previous work [21]. As the soot oxidation patterns differ at high temperatures for the different engine conditions studied here (Figure 2), the calculated activation energies will depend on the temperature range considered for their calculation. When the temperature window is selected from the start of oxidation to 510°C, the activation energy is the same for all the conditions [21]. The results also showed a linear trend being the correlation coefficient greater than 0.98 for all the cases, supporting the validity of the application of the method in this temperature range [21]. For higher temperatures, the weight loss curves diverged from one to another which could be due to the heat transferred from larger exotherm with the larger noEGR sample, compared to the REGR sample. This dependency on the soot mass collected may indicate that, for larger masses, the reaction is partially controlled by diffusion of oxygen [7] and therefore kinetic parameters cannot be determined accurately. Soot was collected on the filter surface forming compact layers one upon the other, and the deeper layers of soot are inaccessible for the oxygen. The slight difference between the activation energies for the three conditions is due to the effect of the different mass loaded: for REGR less mass is available and therefore, a higher noise to signal ratio is produced during TGA.

In addition to the experiments performed by maintaining the same particle loading time, one filter for the baseline condition was loaded for only thirty minutes in order to obtain a comparable particle mass to that loaded in the filter collected under REGR combustion. The filter was introduced in the TG analyser and the same methodology was carried out. In this case, the rate of soot oxidation over the whole temperature range and the MMLRT remained constant for both conditions (Figure 3). Comparing Figures 2 and 3 it was obtained that the sample mass is influencing the soot oxidation behaviour. Therefore, neither EGR nor REGR engine operation significantly affected soot oxidation characteristics, being supported by the soot nanostructure analysis (quantified by interlayer spacing, fringe length and fringe tortuosity) carried out by the authors under the same operating conditions [29]. The activation energy calculated from these conditions also gave similar values to those reported in the literature (i.e. 100 kJ/mol) [21].

Figure 3. Effect of particle mass loading on soot oxidation rate.

2.3.2. Microfiber filter and logarithm method uncertainties

It has been demonstrated that collecting the particles in microfiber filters produces results with a high uncertainty (i.e. low signal to noise ratio) level as the soot mass represents only a small percentage of the total sample mass (i.e. soot and filter material) and the percentage of soot in the total mass affected the soot oxidation profile. Furthermore, the diluted particle sampling conditions in the filter might not be representative for soot oxidation studies compared to those taking place in non-diluted conditions in a particulate filter. Therefore, an alternative method to collect particles, which better simulates exhaust particulate filter conditions, is proposed. The new method allows collection of enough mass of particles without the interferences created by the microfiber filter.

The logarithm method for kinetic analysis of oxidation patterns obtained from heating ramps could lead to erroneous estimations and high variability of the fitting parameters as i) it assumes first-order reaction on the particle mass and oxygen concentration which could be not accurate enough when a deeper kinetic analysis is required, namely, the calculation of the prefactor value A, ii) the optimal range of temperature for calculation is not well defined, iii) buoyancy effects due to the differences in density as the temperature increases [30, 31], iv) the temperature of the sample is not uniformly distributed (i.e. the periphery of the sample will be at lower temperature than the core) and v) mass and thermal inertia can make a difference between the targeted temperature and the actual one inside the furnace [7]. Consequently, an alternative method for kinetic parameter estimation is developed in this work based on the isothermal analysis of GDI soot. It is considered that these issues can be minimised by carrying out isothermal studies. The difference between the furnace wall temperature and the sample is lower during isothermal process and the heating losses are reduced; the sample

temperature is more homogeneous as well as the atmosphere temperature. A detailed description of the method and its comparison with the logarithm method is given in the following sections.

3. DEVELOPING A TGA METHODOLOGY FOR GDI SOOT OXIDATION CHARACTERISATION

3.1. Method development

This new methodology relies on the collection of the particles directly in the raw exhaust stream in the way it is trapped in a vehicle exhaust particulate filter. A monolithic mini-silicon carbide particulate filter (one inch diameter) was cored and sealed from a full size filter. It was then placed into a reactor at 450°C±5°C and soot was loaded using engine exhaust gas at baseline operating condition. The soot in the particulate filter was then removed by blowing purified air into a variable-volume container. In this process, the soot characteristics are thought to be less affected, as there is no need to dilute the exhaust or to prepare the sample for the TGA, and the filter substrate is separated from the soot sample prior the analysis.

In the previous section it was reported that the sample mass played an important role in the results and the MMLRT could be influenced. Therefore, the first analysis carried out was a study of mass effect on the soot oxidation process using the new sampling method (section 3.2). After that, the assumption to apply this method to non-isothermal analysis is validated by studying the heating ramp influence in the kinetic parameters (section 3.3). Finally, an alternative to the logarithm method has been detailed and examined. The reaction orders have been estimated and the errors of assuming order one for both reaction orders have also been calculated (section 3.4). A summary of the parameters modified can be found in Table 5.

Table 5. TGA program

3.1.1. Soot mass effect

The effect of 2 mg, 1 mg and 0.1 mg soot loading in TGA has been examined at 3°C/min heating ramp (Table 5). Two milligrams of soot was chosen as it was found to be the maximum mass that can be introduced in the volume of the pan in TG analyser, while 0.1 mg represents a similar soot mass to that estimated on the soot loaded in the paper filter samples. In addition, an intermediate mass value of 1 mg was also selected for the analysis.

The rate of weight loss is plotted in Figure 4. For E_a calculation, temperatures that produced a loss weight between 90% and 60% were considered due to the better fittings to the proposed model.

Figure 4. Effect of particle mass on soot oxidation rate.

The MMLRT is independent from the mass loaded, especially for the cases of 1 and 2mg, while for 0.1mg there are several local MMLRT caused by the high noise to signal ratio. The activation energy for 1 and 2 mg is around 160 $kJ \cdot mol^{-1}$, while with the 0.1 mg this dropped to 104 $kJ \cdot mol^{-1}$. It is thought that the lower activation energy obtained with the low mass loading is due to the noise for such a small sample, and therefore it cannot be considered as a real value for this condition. It has to be noted that even for 1 mg, the noise is also high and therefore, it would be a better choice to select a sampling mass between 1 mg and 2 mg to avoid this uncertainty and obtain consistent results.

3.1.2. Heating ramp effect

A compromise between the duration of the test and the time for soot oxidation needs to be reached. For the filter TGA test described in section 2.2, and in accordance with the literature, a 3°C/min was chosen to carry out the experiments. However, to complete this study and to investigate in detail the non-isothermal effect in real soot, three heating ramps were selected: 1, 3 and 5°C/min. The results are presented in Figure 5 for 1 and 2 mg to avoid noise interference as concluded previously.

Figure 5. Effect of heating ramp on soot oxidation rate a) 1 mg b) 2 mg.

Higher heating ramp rates shift the oxidation peak to a higher temperature for both mass samples. This is a consequence of the lower available time for the oxidation process to take place at high heating ramp values and therefore, the oxidation temperature continues to increase. This is a typical feature of any kinetic-controlled reaction under non-isothermal conditions (the higher the temperature ramp, the higher the temperatures required to complete the reaction). Indeed, some methods have been proposed in the bibliography to analyse the kinetics of a reaction based on the displacement of the MMLRT under different temperature ramps [32].

As shown previously, the soot oxidation profiles were similar for the different masses at comparable heating ramp conditions, again confirming that sample mass is not a factor under in these experiments.

Figure 6. Effect of heating ramp on soot activation energy: a) 1 mg (solid) b) 2 mg (dashed).

Figure 6, shows the activation energy calculated assuming first-order reaction (logarithm method). Results show that the activation energy decreases with slower temperature ramps, similar to the oxidation temperature trend. The dependence of the soot oxidation patterns and activation energy on

the heating ramp suggests that even a heating ramp of 1°C/min could not be slow enough to give the required isothermal conditions for determining the absolute values of the kinetic parameters. Therefore, the results obtained with this method could be limited to the study of general trends, while the absolute values should be taken with caution. In the following section an alternative method is proposed.

3.2. Exhaustive determination of the kinetic parameters

In order to accurately obtain the values of the kinetic parameters for soot oxidation, such as the activation energy, reaction orders and the prefactor, an isothermal study (section 3.2.1) under different oxygen concentrations (section 3.2.3) has been carried out to avoid the dependence *T-t* when integrating Equation 1. With this objective, the groups of kinetic parameters (*A'*, E_a, and *n*) which minimise the vertical error between the experimental curve obtained from different isothermal TGA and the modelled results obtained from integrating Equation 1 for all the studied temperatures are calculated. An in-house MATLAB program is used for this purpose. The equations implemented in the MATLAB program, Equation 2 and Equation 3, are the result of integrating Equation 1 for different mass reaction orders and considering the initial condition t=0 and mass=100%.

$n = 1$ $$m(t) = 100 \cdot \exp\left(-A \cdot p_{O_2}^r ex\,p\left(-\frac{E_a}{R \cdot T}\right) \cdot t\right) = 100 \cdot \exp\left(-A' \cdot ex\,p\left(-\frac{E_a}{R \cdot T}\right) \cdot t\right) \quad [2]$$

$n \neq 1$ $$m(t) = \left[(1-n) \cdot \left(\frac{100^{1-n}}{1-n} - A \cdot p_{O_2}^r \cdot exp\left(-\frac{E_a}{R \cdot T}\right) \cdot t\right)\right]^{\frac{1}{1-n}} = \left[(1-n) \cdot \left(\frac{100^{1-n}}{1-n} - A' \cdot exp\left(-\frac{E_a}{R \cdot T}\right) \cdot t\right)\right]^{\frac{1}{1-n}} \quad [3]$$

In order to compare the results obtained using different sets of parameters, the root mean square error (RMSE) has been calculated according to Equation 4:

$$RMSE = \sqrt{\frac{1}{t_f}\sum\left(m_{model} - m_{exp}\right)^2} \quad [4]$$

Where t_f is the number of points, m_{model} is the mass obtained using Equations 2 or 3 and $m_{exp}$the data obtained with the TGA respectively.

3.2.1. Isothermal study

The isothermal study enables separation of the temperature and time effects seen in the case of the heating ramps analysis considering that the kinetic equation was originally formulated for infinitesimal isothermal conditions. With this aim, soot samples were heated in nitrogen until the

targeted temperature was attained (400°C, 500°C, 525°C, 550°C, 635°C, 670°C and 750°C), and then the atmosphere in the TG analyser was changed from nitrogen to air (fixed oxygen concentration) for the isothermal process until the weight was stable and close to zero (around 2% ashes were found in this type of sample). The experimental results for the air stage are presented in Figure 7. At 400°C, the weight loss was linear for the 20-hour test. The rate of weight loss was very slow, but it seems that if the sample would have been left enough time, the mass would be completely lost. At 500°C, almost 17 hours were needed to completely oxidise the sample. On the other hand, when the temperature was increased to 635°C, 670°C and 750°C, 100% of the sample was lost in a relatively short time after the targeted temperature was reached. The results for the optimisation are 0.81, $69925 \cdot Pa^{-r}\ s^{-1}$ and 132 $kJ \cdot mol^{-1}$ for the mass reaction order, prefactor (*A'*) and activation energy respectively.

Figure 7. Effect of isothermal analysis on soot oxidation.

3.2.2. Sensitivity analysis

The robustness of the optimal set of values is studied in this section. An analysis of sensitivity has been carried out for the activation energy, prefactor (A') and mass reaction order (n). The rate of variation with respect to the optimum has been calculated whether the variables are varied from -10% to 10% in 5% increments from their optimum value for each variable and recalculating the optimum for that parameter. The results are presented in Figure 8. It can be observed that the activation energy is the parameter which is most affected by the error. A 10% difference in the estimation of the activation energy can lead to an error of 114%. On the other hand, the prefactor is the parameter with which variation produces the lowest error between the experimental and modelled results.

Figure 8. Sensitivity analysis.

Finally, it is important to note that the value of activation energy obtained with the isothermal analysis is lower than those calculated with heating ramps being in agreement with the trend found in the heating ramp study. This confirms that the heating ramp-logarithm method can be used to obtain trends in the activation energy, but the absolutes values overestimate the actual activation energy and slower heating ramps should be performed.

Table 6 presents the group of values which minimised the error i) without assuming any reaction order in r or n (highlighted in green shading) and ii) imposing both reactions orders equal to one (as it is assumed in majority of the literature). Figure 9 shows graphically the difference between the experimental results and the curves obtained when using order one reaction orders. The error induced

assuming both orders equals to the one is 140% larger that the error obtained using the optimal solution. It is important to note that the activation energy is not highly affected by the order of reaction chosen. In fact, whether the logarithm method and the same range of temperatures is used the activation energy is 132 $kJmol^{-1}$, being similar to the value obtained by the simulation with first order reaction assumption. However, the estimated prefactor significantly varies depending on the mass reaction order. Thus, if the only objective is to study the trend of the activation energy depending on different conditions, the logarithm method can be a suitable approach. Finally, it is important to note that the value of activation energy obtained with the isothermal analysis is lower than those calculated with heating ramps being in agreement with the trend found in the heating ramp study. This confirms that the heating ramp-logarithm method can be used to obtain trends in the activation energy, but the absolutes values overestimate the actual activation energy and slower heating ramps should be performed.

Table 6. Optimal values for soot oxidation kinetic parameters

Figure 9. Effect of sample mass and oxygen reaction order on soot oxidation: a) Optimum b) Optimization assuming n=1 and r=1.

3.2.3. Determination of the oxygen reaction order during isothermal analysis at different oxidant concentrations

For the optimal value of the soot mass reaction order and activation energy it was found that several A-r pairs can produce similar values of the error. In Table 7, the simulation results corresponding to the optimised values of the activation energy and the soot mass reaction order while modifying the oxygen reaction order from 0.6 to 0.9 is presented. No restrictions were imposed to the prefactor. As the oxygen reaction order increased the optimised value of A was reduced showing the dependence of these parameters when tests using only one oxygen concentration are analysed. Thus, tests at different oxygen concentrations have been carried out in order to determine the prefactor and oxygen reaction to understand the effect of oxygen concentration on soot oxidation.

Table 7. Alternative *A*-*r* pairs.

Isothermal analysis at 635°C, 670°C and 750°C and three oxygen concentrations: 16.6%, 1.3% and 0.25% in Nitrogen (N_2) were performed. The kinetic parameters obtained are summarised in Table 8. In Figure 10, the experimental results are plotted together with the modelled curves. For 16.6% and 1.3% oxygen concentration, the experimental and theoretical curves correlate well. However, for the lowest oxygen concentration of 0.25%, which is similar to actual oxygen concentration in the exhaust

of gasoline engine, it appears that the form m^n is not able to follow accurately the experimental data and this is leading to the increased error.

Table 8. Optimised kinetic parameters for three oxygen concentrations.

Figure 10. Effect of oxygen concentration on soot oxidation: a) 16.6%, b) 1.3% and c) 0.25%.

4. CONCLUSIONS

A new methodology to obtain the oxidation kinetic parameters of soot emitted from GDI engines is developed. This new methodology involves changes from the current ones in the soot sampling process and thermogravimetric analysis (TGA) as well as in the modelling of the kinetic parameters due to the limitations and/or assumptions widely considered in the state of the art methods.

The GDI engine soot is collected directly in a particulate filter to better reproduce the oxidation process in the actual aftertreatment system as well as to remove the variability in the calculation of the kinetic parameters induced by the large proportion of the microfiber filter in the total mass subjected to the TGA. In contrast to the results from methodologies already available in the literature, in this work, for first time we have identified and eliminated the dependences between mass of the soot loaded in the TGA and its oxidation temperature within the studied range. Furthermore, it was demonstrated that increasing the heating ramp in the TGA the oxidation process was shifted to higher temperatures, trend that was discovered to influence the determination of the kinetic parameters. Therefore, the study is carried out using different isothermal experiments instead of a heating ramp, which produces significantly different values for the kinetic parameters (i.e. activation energy and prefactor).

An exhaustive determination of the kinetic parameters was also developed taking into account the results obtained from the isothermal oxidation TGA. It is concluded that assuming first order reaction can lead to 50% larger error between the Arrhenius-like model and the experimental curve than the optimised model and the prefactor value cannot be taken into consideration. However, the activation energy remained unchanged and was calculated to be 132 $kJ \cdot mol^{-1}$ values that is in agreement with the literature.

ACKNOWLEDGMENTS

The authors would like to thank EPSRC (Grant No: 1377213) and Johnson Matthey for funding the project and providing a scholarship to Maria Bogarra. Innovate UK (Technology Strategy Board) is acknowledged for supporting this work with the project "CO_2 Reduction through Emissions

Optimisation" (CREO: ref. 400176/149) in collaboration with Ford Motor Company, Jaguar Land Rover and Cambustion Ltd. The Advantage West Midlands and the European Regional Development Fund as part of the Science City Research Alliance Energy Efficiency Project are also acknowledged for supporting the research work.

DEFINITIONS, ACRONYMS, ABBREVIATIONS

A'	Exponential prefactor defined as $A' = A \cdot p_{O_2}^r$
A	Exponential prefactor
BMEP	Brake Mean Effective Pressure
bTDC	Before Top Dead Centre
CAD	Crank Angle Degree
DMF	2,5-Dimethylfuran
E_a	Activation energy
EGR	Exhaust Gas Recirculation
Exp	Experimental
GDI	Gasoline Direct Injection
GPF	Gasoline Particulate Filter
IMEP	Indicated Mean Effective Pressure
m	Sample mass
m_{exp}	Mass obtained experimentally
MMLRT	Maximum Mass Loss Rate Temperature
m_{model}	Mass obtained with Arrhenius-like equation
n	Mass reaction order
NEDC	New European Driving Cycle
p_{O_2}	Oxygen partial pressure
PAHs	Polyaromatic hydrocarbons
PFI	Port Fuel Injection
PM	Particulate Matter
r	Oxygen reaction order
R	Universal Gas Constant
REGR	Reformate exhaust gas recirculation
T	Temperature
t	Time
TEM	Transmission Electron Microscope
t_f	Number of points,
TGA	Thermogravimetric Analysis
TWC	Three Way Catalyst
VOC	Volatile Organic Compounds

5. REFERENCES

[1] H. Badshah, I. Khalek, Solid Particle Emissions from Vehicle Exhaust during Engine Start-Up, SAE Int. J. Engines 8 (2015) 1492-1502.

[2] R. Bahreini, J. Xue, K. Johnson, T. Durbin, D. Quiros, S. Hu, T. Huai, A. Ayala, H. Jung, Characterizing emissions and optical properties of particulate matter from PFI and GDI light-duty gasoline vehicles, Journal of Aerosol Science 90 (2015) 144-153.

[3] D.Y.H. Pui, S.-C. Chen, Z. Zuo, PM2.5 in China: Measurements, sources, visibility and health effects, and mitigation, Particuology 13 (2014) 1-26.

[4] T. Mimura, T. Ichinose, S. Yamagami, H. Fujishima, Y. Kamei, M. Goto, S. Takada, M. Matsubara,

Airborne particulate matter (PM2.5) and the prevalence of allergic conjunctivitis in Japan, The Science of the total environment 487 (2014) 493-499.

[5] C.A. Pope, D.W. Dockery, Health Effect of Fine Particulate Air Pollution: Lines that Connect, Journal of the Air & Waste Management Association 56 (2006) 709-742.

[6] K. Donaldson, N. Mills, W. MacNee, S. Robinson, D. Newby, Role of inflammation in cardiopulmonary health effects of PM, Toxicology and applied pharmacology 207 (2005) 483-488.

[7] J. Rodríguez-Fernández, F. Oliva, R.A. Vázquez, Characterization of the Diesel Soot Oxidation Process through an Optimized Thermogravimetric Method, Energy & Fuels 25 (2011) 2039-2048.

[8] I. Atribak, A. Bueno-López, A. García-García, Uncatalysed and catalysed soot combustion under NOx+O2: Real diesel versus model soots, Combustion and Flame 157 (2010) 2086-2094.

[9] A. Bueno-López, Diesel soot combustion ceria catalysts, Applied Catalysis B: Environmental 146 (2014) 1-11.

[10] A. Liati, P. Dimopoulos Eggenschwiler, D. Schreiber, V. Zelenay, M. Ammann, Variations in diesel soot reactivity along the exhaust after-treatment system, based on the morphology and nanostructure of primary soot particles, Combustion and Flame 160 (2013) 671-681.

[11] J. Gao, C. Ma, F. Xia, S. Xing, L. Sun, L. Huang, Raman characteristics of PM emitted by a diesel engine equipped with a NTP reactor, Fuel 185 (2016) 289-297.

[12] J. Gao, C. Ma, S. Xing, L. Sun, L. Huang, Nanostructure analysis of particulate matter emitted from a diesel engine equipped with a NTP reactor, Fuel 192 (2017) 35-44.

[13] L. Chen, Braisher, M., Crossley, A., Stone, R., Richardson D., The Influence of Ethanol Blends on Particulate Matter Emissions from Gasoline Direct Injection Engines, SAE Technical Paper 2010-01-0793 (2010).

[14] D. Uy, M.A. Ford, D.T. Jayne, A.E. O′Neill, L.P. Haack, J. Hangas, M.J. Jagner, A. Sammut, A.K. Gangopadhyay, Characterization of gasoline soot and comparison to diesel soot: Morphology, chemistry, and wear, Tribology International 80 (2014) 198-209.

[15] H. Seong, S. Choi, Oxidation-derived maturing process of soot, dependent on O2–NO2 mixtures and temperatures, Carbon 93 (2015) 1068-1076.

[16] Y. Luo, L. Zhu, J. Fang, Z. Zhuang, C. Guan, C. Xia, X. Xie, Z. Huang, Size distribution, chemical composition and oxidation reactivity of particulate matter from gasoline direct injection (GDI) engine fueled with ethanol-gasoline fuel, Applied Thermal Engineering 89 (2015) 647-655.

[17] C. Wang, H. Xu, J.M. Herreros, T. Lattimore, S. Shuai, Fuel Effect on Particulate Matter Composition and Soot Oxidation in a Direct-Injection Spark Ignition (DISI) Engine, Energy & Fuels 28 (2014) 2003-2012.

[18] C. Wang-Hansen, P. Ericsson, B. Lundberg, M. Skoglundh, P.-A. Carlsson, B. Andersson, Characterization of Particulate Matter from Direct Injected Gasoline Engines, Topics in Catalysis 56 (2013) 446-451.

[19] S. Choi, H. Seong, Oxidation characteristics of gasoline direct-injection (GDI) engine soot: Catalytic effects of ash and modified kinetic correlation, Comb. Flame 162 (2015) 2371-2389.

[20] A. Messerer, R. Niessner, U. Pöschl, Comprehensive kinetic characterization of the oxidation and gasification of model and real diesel soot by nitrogen oxides and oxygen under engine exhaust conditions: Measurement, Langmuir–Hinshelwood, and Arrhenius parameters, Carbon 44 (2006) 307-324.

[21] M. Bogarra, J.M. Herreros, A. Tsolakis, A.P.E. York, P.J. Millington, Reformate Exhaust Gas Recirculation Effect on Particulate Matter, Soot Oxidation and Three Way Catalyst Performance in Gasoline Direct Injection Engines, SAE Int. J. Engines 9 (2016) 305-314.

[22] M. Bogarra, J.M. Herreros, A. Tsolakis, A.P.E. York, P.J. Millington, Study of particulate matter

and gaseous emissions in gasoline direct injection engine using on-board exhaust gas fuel reforming, Applied Energy 180 (2016) 245-255.

[23] G.A. Stratakis, A.M. Stamatelos, Thermogravimetric analysis of soot emitted by a modern diesel engine run on catalyst-doped fue, Combustion and Flame 148 (2003) 249–262.

[24] D. Zhang, Y. Ma, M. Zhu, Nanostructure and oxidative properties of soot from a compression ignition engine: The effect of a homogeneous combustion catalyst, Proceedings of the Combustion Institute 34 (2013) 1869-1876.

[25] M. Salamanca, F. Mondragón, J.R. Agudelo, P. Benjumea, A. Santamaría, Variations in the chemical composition and morphology of soot induced by the unsaturation degree of biodiesel and a biodiesel blend, Combustion and Flame 159 (2012) 1100-1108.

[26] B. Dernaika, D. Uner, A simplified approach to determine the activation energies of uncatalyzed and catalyzed combustion of soot, Applied Catalysis B: Environmental 40 (2003) 219–229.

[27] J. Gao, C. Ma, S. Xing, L. Sun, Oxidation behaviours of particulate matter emitted by a diesel engine equipped with a NTP device, Applied Thermal Engineering 119 (2017) 593-602.

[28] A. Yezerets, Currier, N., and Eadler, H., Experimental Determination of the Kinetics of Diesel Soot Oxidation by O2 - Modeling Consequences, SAE Technical Paper 2003-01-0833 (2003).

[29] M. Bogarra, J.M. Herreros, A. Tsolakis, A.P.E. York, P.J. Millington, F.J. Martos, Influence of on-board produced hydrogen and three way catalyst on soot nanostructure in Gasoline Direct Injection engines, Carbon 120 (2017) 326-336.

[30] J. Rodríguez-Fernández, J.J. Hernández, J. Sánchez-Valdepeñas, Effect of oxygenated and paraffinic alternative diesel fuels on soot reactivity and implications on DPF regeneration, Fuel 185 (2016) 460-467.

[31] M.E. Brown, Introduction to thermal analysis techniques and applications, Springer Publishers, New York 2004.

[32] P.E. Sánchez-Jiménez, J.M. Criado, L.A. Pérez-Maqueda, Kissinger Kinetic Analysis of data obtained under different heating schedules, Journal of Thermal Analysis and Calorimetry 94 (2008) 427–432.

Figures

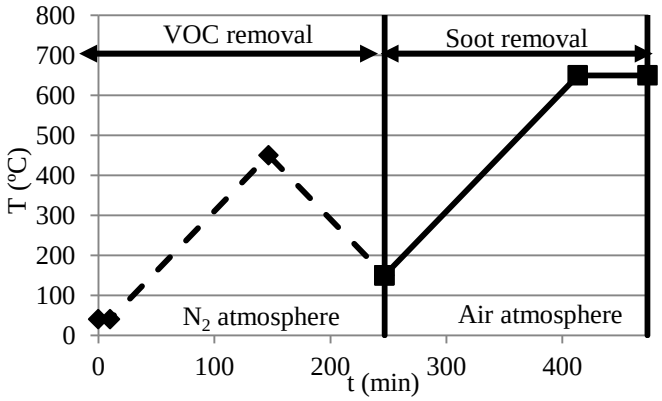

Figure 1. TGA program.

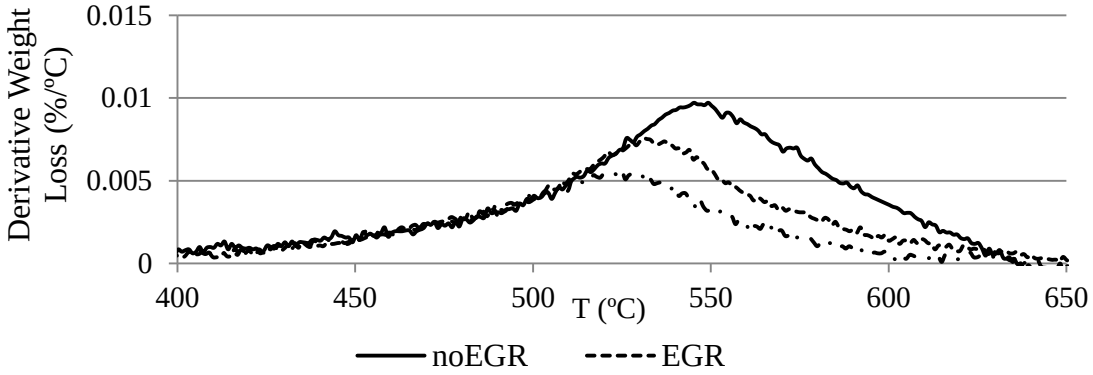

Figure 2. Effect of EGR and REGR on soot oxidation rate in TGA.

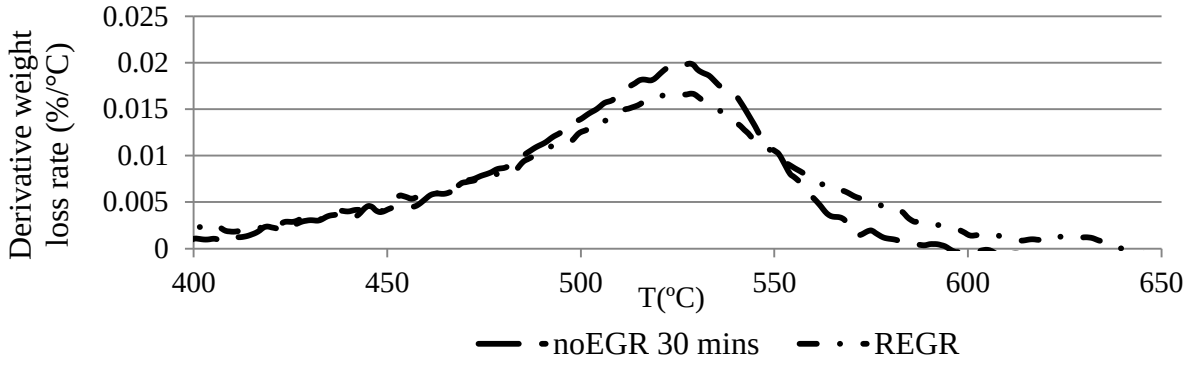

Figure 3. Effect of particle mass loading on soot oxidation rate.

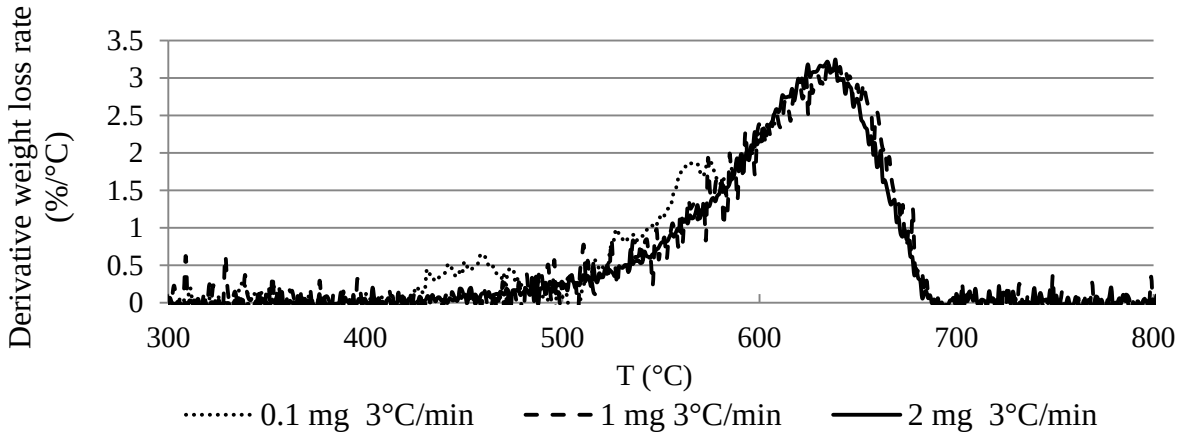

Figure 4. Effect of particle mass on soot oxidation rate.

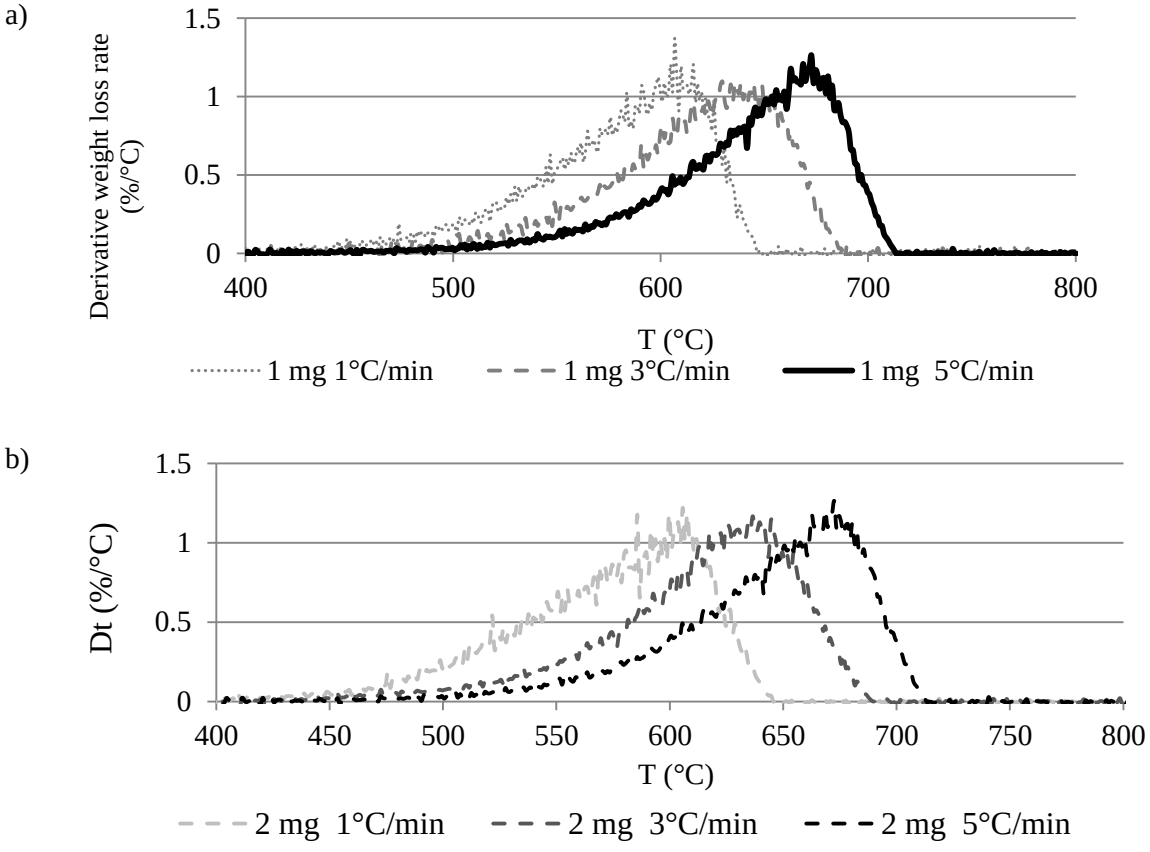

Figure 5. Effect of heating ramp on soot oxidation rate a) 1 mg b) 2 mg.

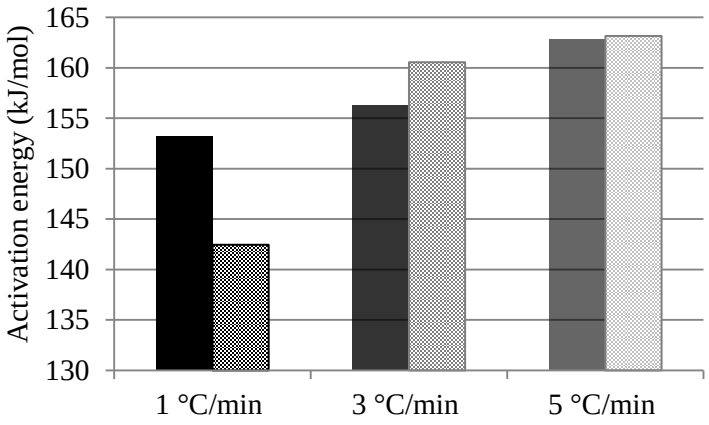

Figure 6. Effect of heating ramp on soot activation energy: a) 1 mg (solid) b) 2 mg (dashed).

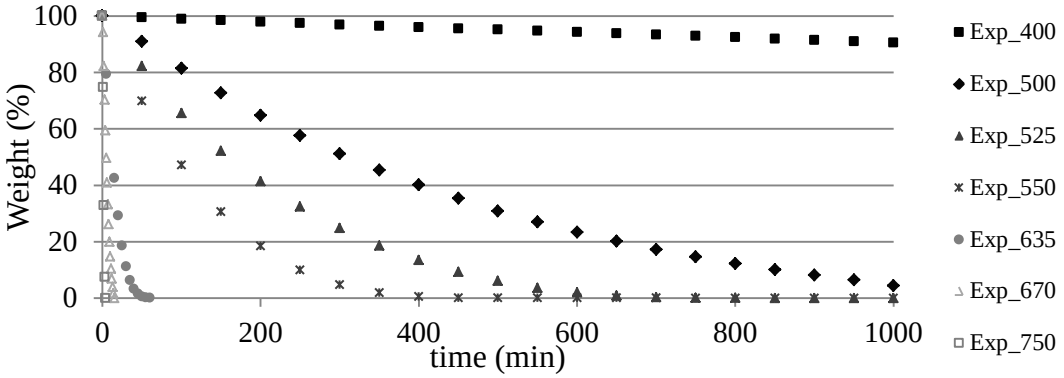

Figure 7. Effect of isothermal analysis on soot oxidation.

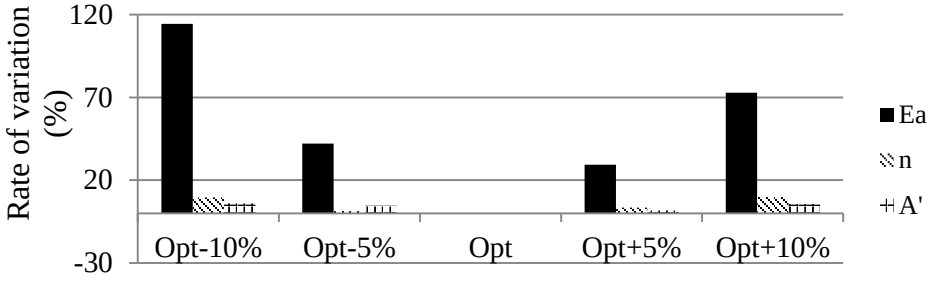

Figure 8. Sensitivity analysis.

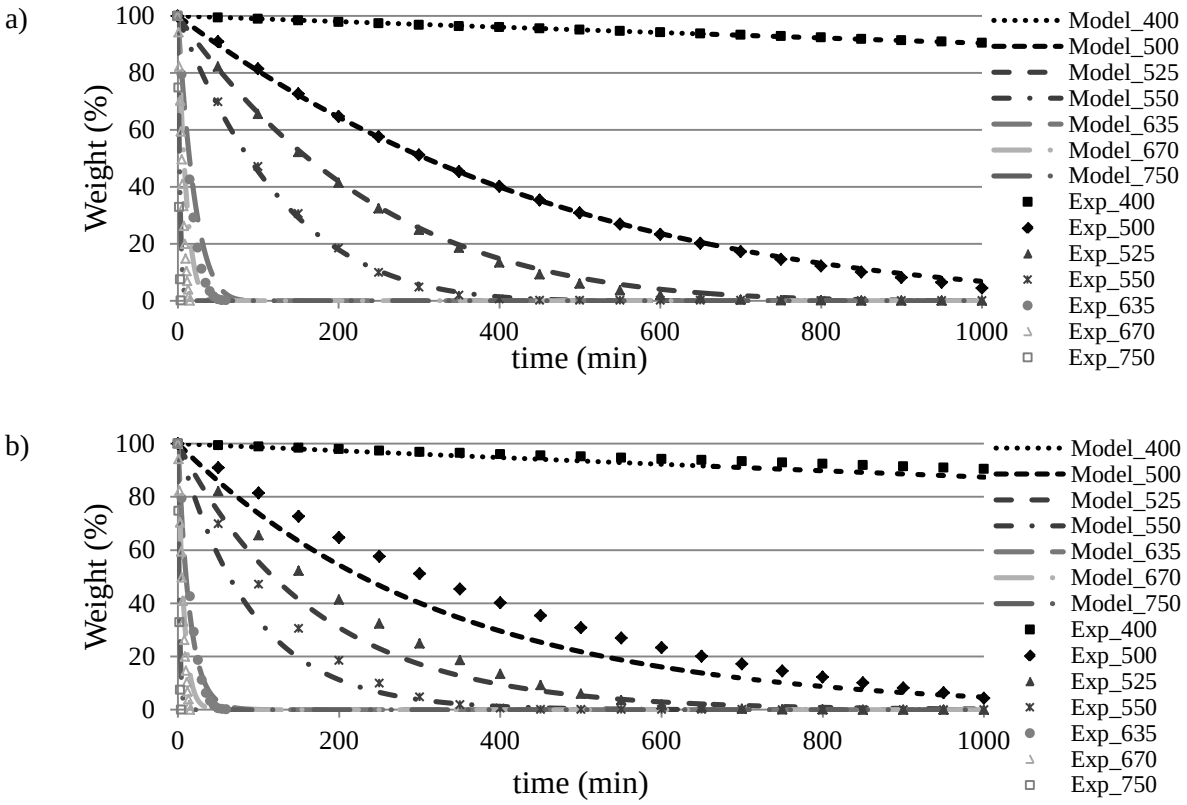

Figure 9. Effect of sample mass and oxygen reaction order on soot oxidation: a) Optimum b) Optimization assuming n=1 and r=1.

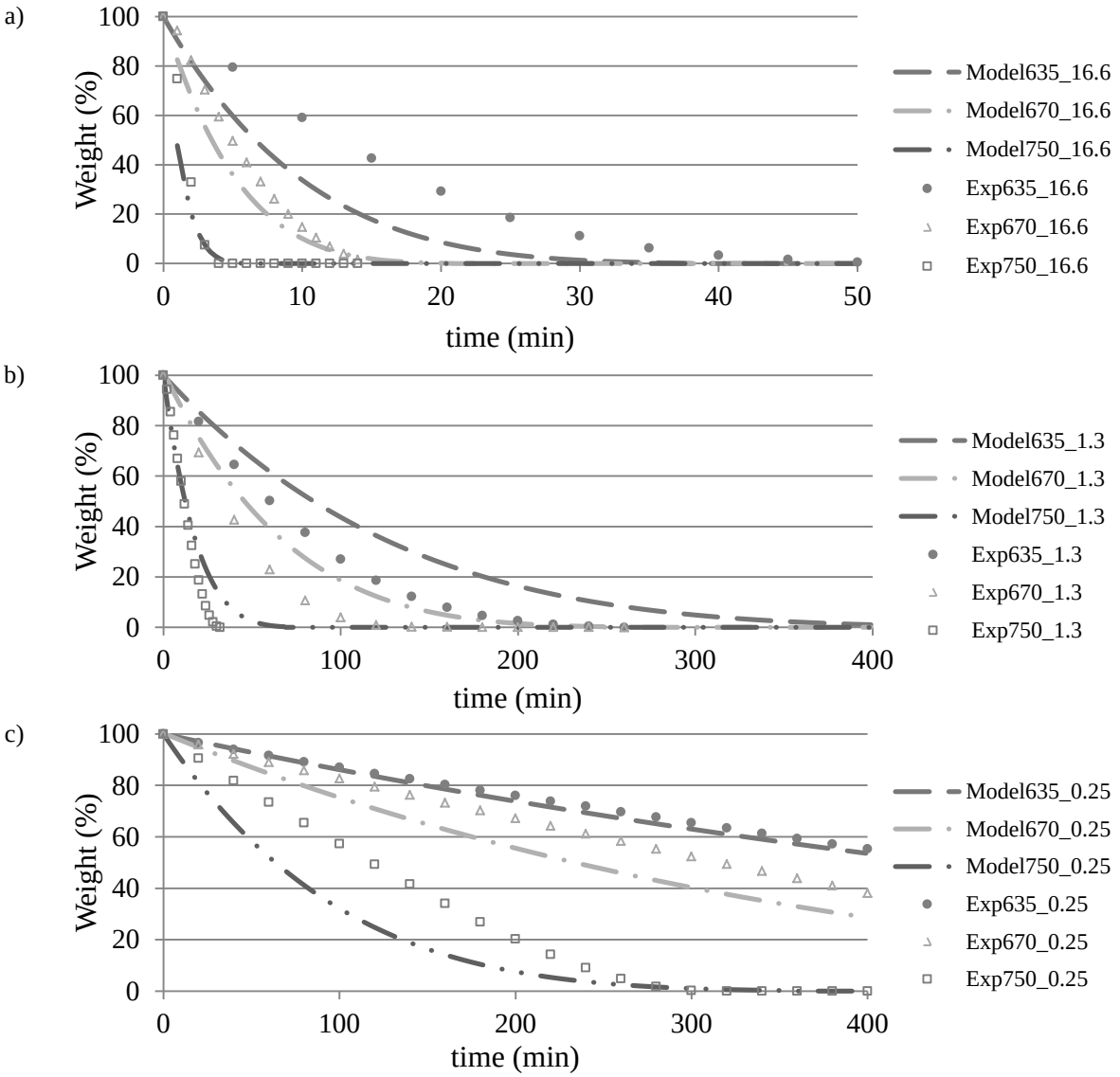

Figure 10. Effect of oxygen concentration on soot oxidation: a) 16.6%, b) 1.3% and c) 0.25%.

Table 1. Summary of the kinetic parameters found in the literature.

Ref.	Engine condition	Fuel	E_a (kJ mol^{-1})	A' (s^{-1})	n	r	Collection method	TGA method
[16]	1500 rpm,10.6 bar BMEP	**Gasoline**	**197**	- - -	1*	1*	Peeled off from the Quartz filter	Mass sample: 5mg Nitrogen atmosphere: 3°C min^{-1}, isothermal 30 minutes at 400°C Air atmosphere: 30°C min-1 to 800°C
		E10	183					
		E20	163					
	1500 rpm,14.2bar BMEP	**Gasoline**	**234**					
		E10	215					
		E20	174					
	3000 rpm, 10.6 bar BMEP	**Gasoline**	**256**					
		E10	217					
		E20	171					
	3000 rpm,14.2 bar BMEP	**Gasoline**	**235**					
		E10	221					
		E20	189					
[17]	1500 rpm 5.5 bar IMEP SOI= 100 CAD bTDC λ=0.9	**Gasoline**	**131**	- - -	1*	1*	Cut from Micro- glass filters	Mass sample: >0.044mg Nitrogen atmosphere: 30°C min^{-1}, isothermal 20 minutes at 500°C Air atmosphere: 3°C min^{-1} to 700°C
		DMF	109					
	1500 rpm 8.5 bar IMEP SOI= 100 CAD bTDC λ=0.9	**Gasoline**	**153**					
		E25	124					
		Ethanol	83					
[18]	Urban part of the NEDC cycle	Gasoline	146	The value of A is dependent on the mass left	1*	0.5 to 1**	Uncoated aluminium titanate filter (after TWC)	TPO Three levels of oxygen (8, 14.5 and 21 vol%) Heating ramps (1,2, 3°C min^{-1}) and NO_2 (500, 1000 and 1500 ppm) Isothermal analysis at 463, 488, 489 and 511°C 21% O_2
		Ethanol	71					
[19]	Cold start	Gasoline	127	16594.1	0.982**	- - -	Scraping off Teflon-filters	Isothermal studies at 500, 550, 600 and 650°C Non-isothermal: Nitrogen atmosphere: 30°C min^{-1}, isothermal 30 minutes at 600°C O_2-containing atmosphere (8%): 1°C min^{-1} to 900°C
	1250 rpm 25% load SOI= 330 CAD bTDC. Engine out		125	13503.4	0.778**			
	1250 rpm 25% load SOI= 330 CAD bTDC. TWC out		132	34234.9	0.512**			
	1500 rpm 50% load SOI= 330CAD bTDC		142	126880.4	1.011**			
	1500 rpm 50% load SOI= 330 CAD bTDC with subsequent 20 times of fuel-cut operation Idle (engine start ~1 min)		127	15582.4	0.976**			

* Assumed ** Calculated

Table 2. Engine specifications.

Compression Ratio	10:1
Bore x Stroke	87.5 x 83.1 mm
Turbocharger	Borg Warner K03
Rated Power	149 kW At 6000 rpm
Rated Torque	300 Nm at 1750-4500 rpm
Engine Management	Bosch Me17

Table 3. Gasoline properties.

Analysis (Test method)	Result
Density at 15ºC (kg/m^3)	743.9
IBP (ºC)	34.6
20% v/v (ºC)	55.8
50% v/v (ºC)	94.0
FBP (ºC)	186.3
C m/m %	84.16
H m/m %	13.48
O m/m %	2.36
Paraffins (% vol)	43.9
Olefins (% vol)	11.7
Naphthenes (% vol)	7.8
Aromatics (% vol)	26.9
Oxygenates (% vol)	7.7
Sulfur (ppm)	6
Lower calorific value (MJ/kg)	42.22
MON	85.3
RON	96.5

Table 4. TGA program.

Step	**Action**
1	Initial Atmosphere: Nitrogen
2	Hold for 10 min at 40°C
3	Heat from 40°C to 450°C at 3.00°C/min
4	Cool from 450°C to 150°C at 3.00°C/min
5	Changing Atmosphere: Air (21% O_2)
6	Heat from 150°C to 650°C at 3.00°C/min
7	Hold for 60 min at 650°

Table 5. TGA program

Parameter	Value
Mass	~2 mg ~1 mg ~0.1 mg
Final temperature	Up to 800°C
Oxidation heating ramps	1.00°C/min 3.00°C/min 5.00°C/min

Table 6. Optimal values for soot oxidation kinetic parameters

Case	n	A' ($Pa^{-r}\cdot s^{-1}$)	E_a ($kJ\cdot mol^{-1}$)	RMSE	Rate of variation (%)
a)	0.81	69925	132	4.3	-
b)	1	84100	138	10.3	140

Table 7. Alternative *A*-*r* pairs.

r	A'($Pa^{-r}\cdot s^{-1}$)	RMSE
0.6	70004	4.3
0.7	69915	4.3
0.8	69672	4.3
0.9	69925	4.3

Table 8. Optimised kinetic parameters for three oxygen concentrations.

n	0.81
r	1
A ($Pa^{-1}\cdot s^{-1}$)	7
E_a ($kJ\cdot mol^{-1}$)	130